



**HAL**  
open science

## Deceleration measurement for penetration into steel target

Wendong Zhang, Jijun Xiong, Lujiang Chen, Youchun Ma, Zhi-Qiang Feng

► **To cite this version:**

Wendong Zhang, Jijun Xiong, Lujiang Chen, Youchun Ma, Zhi-Qiang Feng. Deceleration measurement for penetration into steel target. 5th WSEAS International Conference on Instrumentation, Measurement, Circuits and Systems, Apr 2006, Hangzhou, China. pp.677-683. hal-01179054

**HAL Id: hal-01179054**

**<https://hal.science/hal-01179054>**

Submitted on 2 Jul 2018

**HAL** is a multi-disciplinary open access archive for the deposit and dissemination of scientific research documents, whether they are published or not. The documents may come from teaching and research institutions in France or abroad, or from public or private research centers.

L'archive ouverte pluridisciplinaire **HAL**, est destinée au dépôt et à la diffusion de documents scientifiques de niveau recherche, publiés ou non, émanant des établissements d'enseignement et de recherche français ou étrangers, des laboratoires publics ou privés.

# Deceleration Measurement for Penetration into Steel Target

Wendong Zhang[1], Jijun Xiong[1], Lujiang Chen[1], Youchun Ma[1], Zhi-Qiang Feng [2]

<sup>1</sup>Key Lab on Instrumentation Science & Dynamic Measurement of the Education Ministry of China, North University of China, Taiyuan 030051, China

<sup>2</sup>Laboratoire de Mécanique d'Evry (CEMIF-IME), Université d'Evry-Val d'Essonne, 40 rue du Pelvoux, 91020, Evry, France

*Abstract:* - Deceleration measurement is both very important and very difficult for the research on the penetration. This paper presents an ultra-high g deceleration measurement experiment. In the experiment, penetration occurs while a tungsten alloy projectiles with velocity of 573m/s impacts a 50-mm-thick steel target. Numerical simulation utilizing ANSYS/LS\_DYNA is carried out firstly to estimate the deceleration value and its duration time, and followed by the detail description to the design of the measurement device. Experiment results show that more than 145,000g deceleration value is measured. The results are consistent with the simulation ones. However, compared to theoretical analysis result of a previously published penetration model, the experiment result shows some disparities.

*Key-Words:* - penetration; steel target; deceleration-time measurement; high g; numerical simulation

## 1 Introduction

Research on penetration is significant for the deceleration measurement. Penetration and perforation processes for various targets are very complex. People have conducted a large number of studies on penetration mechanism. The deceleration measurement is necessary to verify various theoretical models and numerical simulation results. The responses of projectiles and targets with concrete [1-3] and rock [4] targets, the projectiles loss small amounts of mass through abrasion and experienced relatively small deformations. Therefore, rigid-body deceleration data provide a measure for net force on the projectile nose during the penetration event. However, most experimental studies [1-7] only provide penetration depth versus striking velocity data, and deceleration data are limited.

Ultra-high g deceleration measurement is very difficult. Many measurement technologies for penetration have been developed. Byers, et al. [8] conducted a penetration experiment for lakebed target with striking velocity of 300m/s, which had accelerometer and radio telemetry structurally mounted within the projectile. Radio telemetry sent the deceleration signal from accelerometer during penetration. Henceforth, radio telemetry technology got improved and digital storage technology was developed, could recover the deceleration signal from a memory chip within the projectile. By means of this method, Forrestal and Luk [9] reported deceleration data for six experiments into soil targets with peak rigid-body decelerations of about 1,200g, which was lower due to the soft targets. For the reported tests of penetration with more resistant concrete targets [10], Forrestal and Frew reported peak rigid-body decelerations between 6,000 and

13,000 g. Researchers of Sandia developed a single channel high-shock data recorder in 1999 [11], which could survive under the overloading range of 40,000g. The Munitions Experimental Test Centre (METC) of Canada designed the three channel high-g recorder in 2002, which could withstand overloading of 100,000g. Since 1984, Wendong Zhang, et al. were engaged in the study of the storage measurement technology. Wendong Zhang, et al. [12] presented the intelligent missile black-box, which could work against overload of 20,000g. Also, Wendong Zhang [13] reported the deceleration data for over ten experiments into concrete targets with the anti-overloading value of 50,000 g.

In this paper, an ultra-high g deceleration measurement experiment was presented to study the penetration into steel target. A numerical simulation utilizing ANSYS/LS\_DYNA was carried out to predict the penetration situation with the same penetration condition. The design of the deceleration measurement device was explicated. Full scale of the measured deceleration is 160,000g. In addition, we compared the experiment result with theoretical ones obtained from a previous model published by Q.M. Li. et al [14-15].

## 2 Experiment description

We had conducted a penetration experiment into a single 50mm-thick target. A 100-mm-diameter, smooth-bore power gun launched the 28.7 kg projectile with striking velocity of about 573m/s. The projectile was fitted with the sabots and the obturators that separated from the projectile prior to impact. The multilayer general steel plates and the concrete recovery device were located in the experimental field. The distance between gun and

target was 20m. The device was installed in the tail of projectile. The projectile geometries and accelerometer location were shown in Fig.1. The projectile was machined from tungsten alloy and parameters are shown in table 1. The target was machined from 1016 steel.

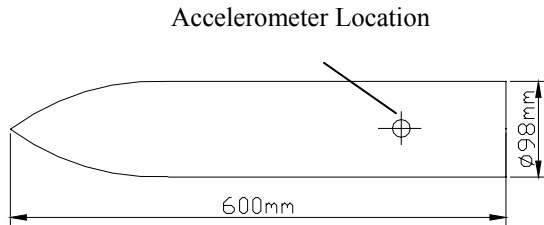


Fig.1 Projectile geometries and accelerometer location

Table.1 parameters of projectile

Material	Mass	Shape	CRH
Tungsten alloy	28.7kg	Ogive-nose	3.0

Projectile striking velocity was measured with a fixed distance measurement. This measurement was as follows: Wire nettings stationed at two locations along the flight path near the power gun, and connected with a test circuit; when the projectile flight through the wire nettings, the circuit detected two signal impulses and calculated the time between two impulses; then, the striking velocity was obtained.

For the aspect of circuit design, the full-scale range of  $\pm 160,000$  g and the triggering threshold value of 30,000 g were set in this experiment. When accelerometer was subjected to 30,000g overloading, the device recorded the data in the time of 1s both before triggering and after triggering. In this way, acceleration during launch and deceleration during the penetration were recorded. Finally this device was retrieved reliably.

Successful experiment also depends on the selection of high g accelerometer. The piezoelectric thin film high-g accelerometer was selected, which was developed by Beijing Institute of Technology in China. Table 2 showed parameters of this accelerometer, which indicated almost the same characteristics as the Endenco 7270A-200K.

Table.2 parameters of accelerometer

Frequency response	Linear range(g)	Sensitivity(mV/g)	Impact limit(g)
0~150000Hz	180000	0.001	180000

### 3 Estimation of deceleration

Prior to the test, numerical simulation utilizing ANSYS/LS\_DYNA was carried out to analyze the above process. The Lagrangian approach was used for simulation. Both projectile and target adopted the elastic and kinematic plastic hardening material model \*MAT\_PLASTIC\_KINEMATIC in ANSYS/LS\_DYNA, as it was applicable to the low-velocity penetration. Material properties of the model materials are shown in table 3.

Table.3 Material properties of the model materials

Material	DENS (kg/m <sup>3</sup> )	E(G Pa)	NUX Y	Yield Stress(MPa)	Tangent Modulus(MPa)
Tungsten alloy	17600	350	0.284	785	1180
1016 steel	7865	200	0.27	310	763

Considering the edge reflection effect of target wave, target dimension was 1000mm  $\times$  1000mm, 50mm-thick. Because of the structural symmetry, only one quarter of the geometry was modeled to reduce the computational time. Fig. 2 showed the finite element discretization of the projectile and the target. By means of the adaptive meshing, the projectile was meshed into 14400 8-node hexahedron solid elements, and the target, 5445 elements. The time step was 5ms (the time required for the projectile to perforate through the target) and the termination was 4 $\mu$ s (depending on the sampling rate of 250 kHz). The ERODING\_SURFACE\_TO\_SURFACE (ESTS) contact was used after each time step. The contact stiffness scale factor was assigned the value 1.0. The striking velocity of 573m/s was constant before penetration of target, so initial distance between projectile and target was set as 0.1m.

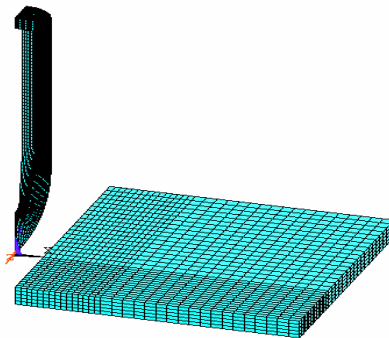


Fig.2 Finite element discretization of the projectile and the target

The simulation results of curves of penetration into steel target by Tungsten alloy projectile could be seen in Fig.3, Fig.4 and Fig.5 respectively. Fig.3 was the deceleration-time curve, Fig.4 was velocity-time curve and Fig.5 was displacement-time curve.

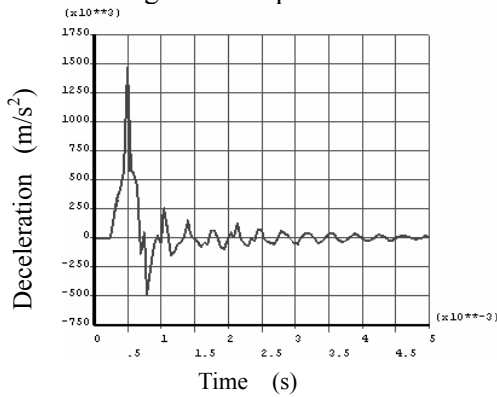


Fig.3 Deceleration-time curve of penetration into steel target by Tungsten alloy projectile

As we could see in Fig.3, at the beginning of the penetration, the deceleration-time data rised sharply to a peak value, and then there was a sudden decrease of data. Resistance brought to bear on projectile was greatly reduced because of the damage and tension failure of target material surrounding the projectile's tine. Furthermore, there was a shaking phenomenon during the interaction between projectile and target. The shaking phenomenon was caused by the compressive stress waves generated in both the projectile and the target. For subsonic impacts these waves propagate at the sound speed of the materials and at the shock speed for impacts at hypervelocity. These are followed by slower moving shear waves. The two waves propagate until they interact with a free surface from which a compressive wave is reflected as a tensile pulse, and material failure by a variety of mechanisms can occur, see Ref. [16]. Fig.3 showed the peak deceleration-time of 150,000 g and the peak duration time of about 400 $\mu$ s. From Fig.4 and Fig.5, the residual velocity was 420m/s and the

displacement during the penetration was 0.186m.

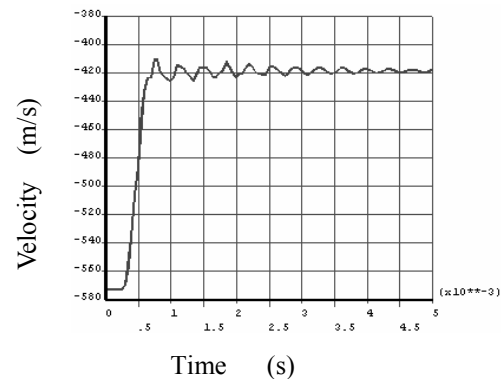


Fig.4 Velocity-time curve of penetration into steel target by Tungsten alloy projectile

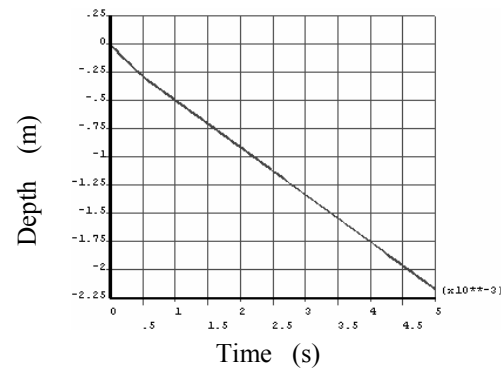


Fig.5 Displacement-time curve of penetration into steel target by Tungsten alloy projectile

#### 4 The ultra-high g deceleration measurement device

The ultra-high g deceleration measurement device was mainly composed of an accelerometer, an acceleration data recorder, protective equipment and data processing equipment. The operating principle was as follows: First, the device was mounted within the projectile before launch; and then during the penetration, the device acquired and stored the real-time dynamic penetration signal of the projectile; after the penetration, the projectile was recovered from the target, and the recorded data was retrieved

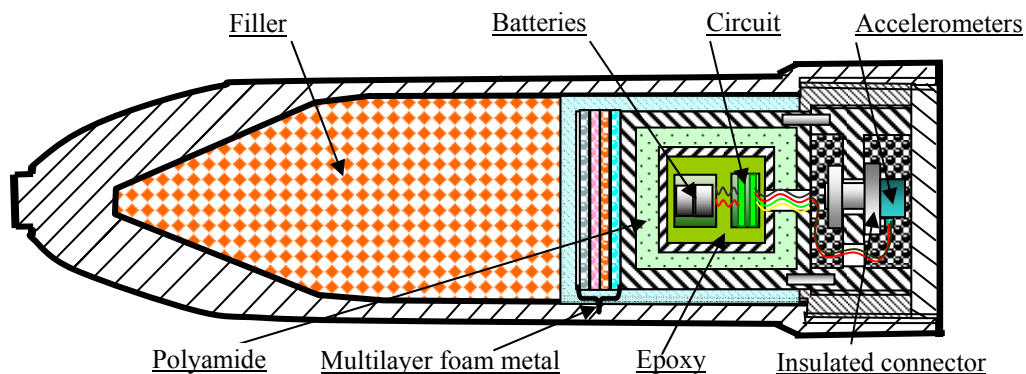


Fig.6 Cross-section of high g deceleration measurement device embedded in the projectile

from the recovered device and processed through data processing equipment. And the device could be reused.

#### 4.1 Design of systematic structure

The cross-section of high g deceleration measurement device embedded in the projectile was shown in Fig.6. It included an accelerometer, an acceleration data recorder and protective equipment. The recorder directly obtains signal from the accelerometer during the course of penetration and accomplishes the signal matching, A/D, transforming, coding and storing, followed by transmitting the processed result to data processing equipment. Protective equipment ensured this device work well under harsh environment, such as high-g overload, high shock and transient high temperature. Deceleration data recorder and accelerometer with high range were connected rigidly by insulated connector and signal wires and mounted within the projectile together.

According to the simulation result, for the deceleration and other correlation parameter measurements during penetration into hard targets with high velocity (between 550m/s and 1,000m/s), the feasible design of protective equipment provided a reliable safeguard for the deceleration data recorder. Integrative protection technology with the suspending and multilevel shockmitigation structure was adopted in protective equipment. Specific execution method was as follows: the circuit system of the recorder was encapsulated by epoxy resin, forming the integrative style of electronics module; then the integrated electronics module was packaged by polyamide foam that had certain elasticity and hardness in a rigid shell, which was called the suspending structure of spring capability. Epoxy resin and polyamide foam had been commonly considered as good protective material to mitigate shocks. They could attenuate impulsive forces and most impact energies during the penetration were

reflected or absorbed [12]. In addition, the application of different metal foam (aluminum foam and copper foam) [17, 18] with the non-linear and good cushion properties also achieved protective function effectively, which could also absorb some inertia energies.

#### 4.2 Deceleration data recorder

Deceleration data recorder was the key device for the deceleration measurement. As shown in Fig.7, the block principle diagram of high g deceleration data recorder was composed of the analog signal process circuit, 12 bit A/D converter, time-base circuit, crystal oscillator, power module, reset circuit, logic control center with CPLD integrated unit, SRAM and interface circuit. In the recorder, logic control center adopted the modular design, which mainly included control module, address generator, trigger module, negative delay counter, frequency dividing module and 12 bit parallel to serial shift register. Among them, control module mainly realized most control functions, such as A/D read-write, memory read-write, sampling, intelligent power and indicator light switching and so on.

After the projectile with the device was launched, the data acquisition and storage module started to work under the system start-up instruction. Measured signal gained from accelerometer converted to the quantity of electric charge, which changed into a voltage signal through signal process circuit. Then the sampling circuit started to collect data by A/D converter as soon as the writing signal was enabled, and sampling data were written into SRAM timely under the control of the address signal and writing enable signal. Meantime, the voltage signal was connected with exterior trigger circuit. When it exceeded the trigger voltage, trigger signal was generated immediately. Herewith, the principle of negative time delay applied to the circuit design, using the characteristic signal generated from accelerometer during penetration to control the recording state automatically.

After reliable recovery of the device, recorded data

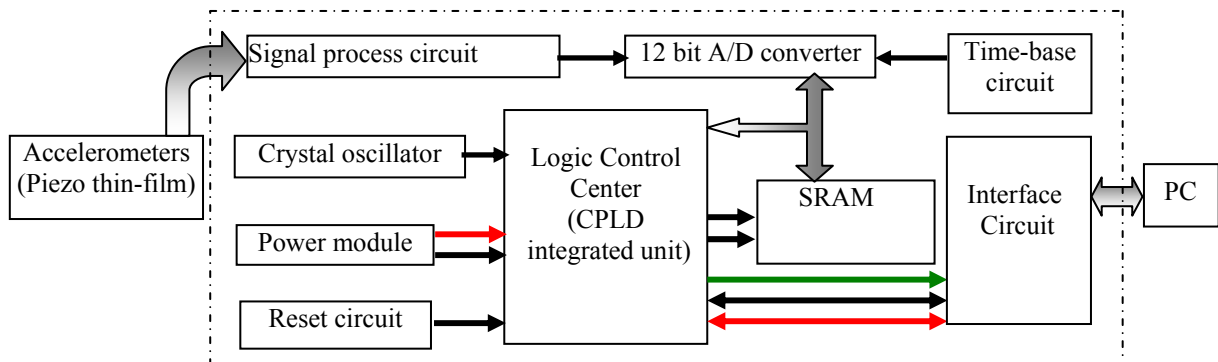


Fig.7 Block diagram of high g acceleration recorder's principle

would be transferred to PC through a parallel interface circuit and the matching software, to reproduce the deceleration-time signal. The deceleration data recorder was powered by a power intelligent control module to keep work well and preserved the data for one year at least.

The previous research showed that the miniature structure of higher intensity and rigidity was good. It had good anti-overload and anti-shock properties under high-frequency vibration and shock excitation. Therefore, micromation and low power consumption were mainly considered in the design of high g deceleration data recorder. Major technological approaches were as follows: 1) the integration of logic control circuit with CPLD (complex programmable logic device); 2) application of the BGA/CSP potted element and micro-SMD component; 3) the design of power intelligent control, to reduce the power consumption time factor under the waiting-triggering or data retention state. Power of components without state holding and data retention should be switched off as much as possible, correspondingly accomplishing the design of low-power consumption efficiently; 4) to make circuit dimension further reduced, the smaller batteries were adopted in the low power consumption design.

Circuit system and deceleration data recorder were shown in Fig. 8 and Fig.9 respectively. Technical parameters of this device were follows: single channel, the memory capacity 4Mb, the sampling rate 250 kHz, recording time 2s, whole dimension less than 10 cm<sup>3</sup>. Waiting state power consumption was only about 18  $\mu$ A, and the operating power consumption was no more than 8mA.

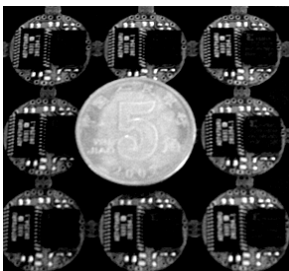


Fig.8 Circuit system

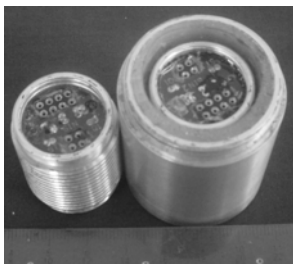


Fig.9 Deceleration data recorder

## 5 Experimental Results



Fig.10 Post-experiment site



Fig.11 The retrieved data recorder

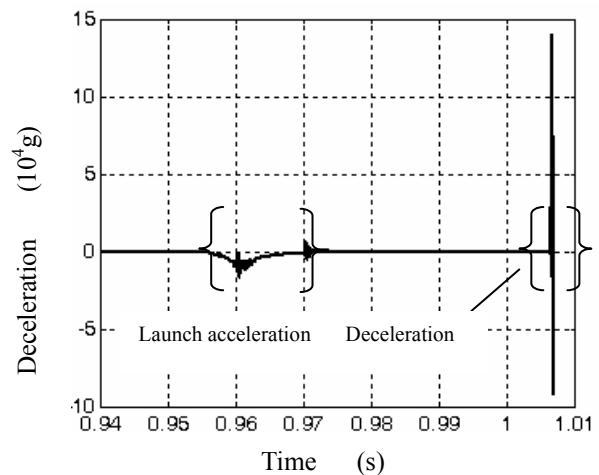


Fig.12 Launch acceleration in the bore of the gun and deceleration during the penetration

The results of ultra-high g deceleration measurement experiment were given in Fig.10, Fig.11 and Fig.12. Fig.10 showed post-experiment site. The projectile deformed at impact, eroded during the penetration process and finally perforated the target. The retrieved projectile lost small amounts of mass through abrasion and experienced relatively small deformations. The slight deformations were near the nose and some shank bending. It confirmed that the assumption of rigid projectile had experimental basis for the research on the low-velocity penetration. Fig.11 indicated the retrieved acceleration data recorder. It was in good condition and un-deformation. Fig.12 showed launch acceleration

in the bore of the gun and deceleration during the penetration.

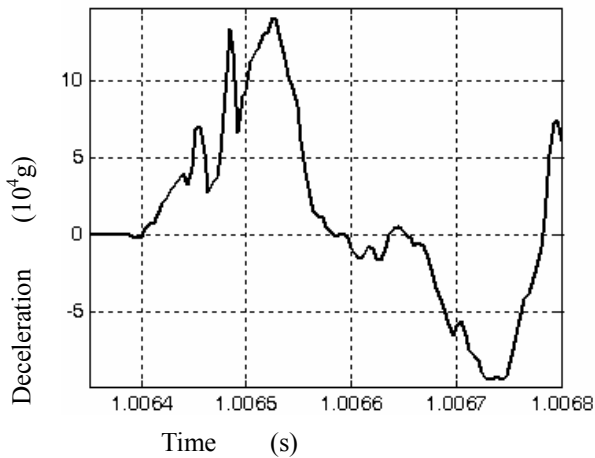


Fig.13 Deceleration-time curve during the penetration

The whole process from launching to penetration with 50mm target was recorded by this device. Fig.12 indicated that the time difference between gun muzzle and target was about 36ms, which agreed with the required time during the 20m-distance flying with an average velocity of 573m/s. It also reflected the force state of projectile. Integration of measured launch acceleration-time data was performed to obtain striking velocity of 617m/s. Fig.13 presented deceleration-time curve during the penetration (partial enlarged view of Fig. 12), the peak of which was up to 145,000 g and the duration time was about 200 $\mu$ s. The negative overload caused by shocking during penetration also reached 93,680 g and its duration time was about 150 $\mu$ s. From Fig.14 and Fig.15, integrations of measured deceleration-time data were performed to obtain velocity and penetration depth. These indicated that the residual velocity was 462m/s and the displacement during the penetration was 0.152m. Table 4 summarized the simulation results and experiment results and indicated that the experimental results were in good agreement with simulation results.

Table.4 simulation results and experiment results

Result	Striking velocity (m/s)	Residual velocity (m/s)	Peak value (g)	Duration time ( $\mu$ s)	Displacement during the penetration (m)
Simulation	573	420	150,000	400	0.186
Experiment	617	462	145,000	200	0.152

## 6 Comparison with theoretical analysis result

In this section, the experimental result of penetration for a steel target was compared with the theoretical prediction result from a mathematic model [14, 15] for penetration with rigid, ogive-nose projectiles, presented by Chen, et al. of UMIST. The penetration equations were guided by cavity expansion theory. The axial resistant force on the projectile nose is determined by:

$$F_x = \frac{\pi d^2}{4} (A \sigma_y N_1 + B \rho V^2 N_2)$$

$$A = \frac{2}{3} \left\{ 1 + \ln \left[ \frac{E}{3(1-\gamma)\sigma_y} \right] \right\}$$

Where  $d$  is the calibre diameter of projectile shank. And  $\rho$ ,  $\sigma_y$  are yielding stress and density of the target material respectively.  $E$  is elastic modulus.  $A$  and  $B$  are dimensionless material constants of target materials.  $N_1$  and  $N_2$  are two dimensionless parameters related to the nose shape and friction coefficient. Formulae of  $N_1$ ,  $N_2$  and  $N^*$  for ogive nose can be found in Chen and Li [14]. If the friction is ignored ( $\mu=0$ ),  $N_1=1$ ,  $N_2=N^*$ . The penetration depth  $X$  is determined by:

$$M \frac{dV}{dt} = -F_x \quad \text{and} \quad V = \frac{dX}{dt}$$

With the initial condition  $V(t=0) = V_i$  and  $X(t=0) = 0$ .

The dynamics penetration process was very complex, and the prediction of penetration model depends on many factors. The deceleration-time history during the penetration could not be predicted directly with this model. Therefore, integrations of measured deceleration-time data were performed to obtain velocity and displacement. Thus, we could compare velocity from the model prediction ( $B=1.0$ ,  $\mu=0$ ) with an integration of the measured deceleration-time data in Fig.14, and we could also compare displacement on the above condition with a double integration of the measured deceleration-time data in Fig.15. The comparison showed these results had nearly the same trend. The model predictions were in good agreement with the rigid-body responses before the rise time of about 80 $\mu$ s, and the relative error was less than 10%. However, the model predictions deviated from the data after the penetration time of about 80 $\mu$ s.

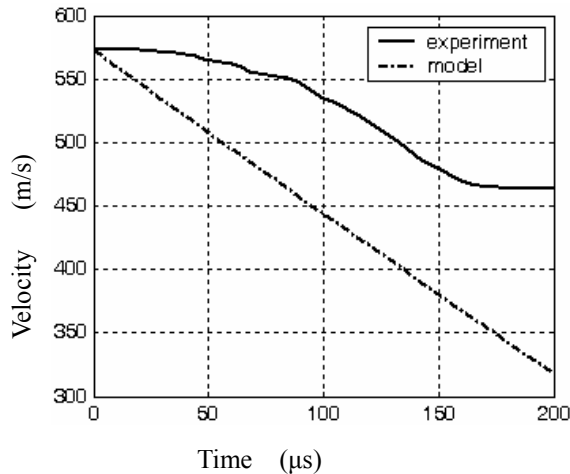


Fig.14 Velocity versus time data and model prediction,  $B=1.0$ ,  $\mu_m=0$ .

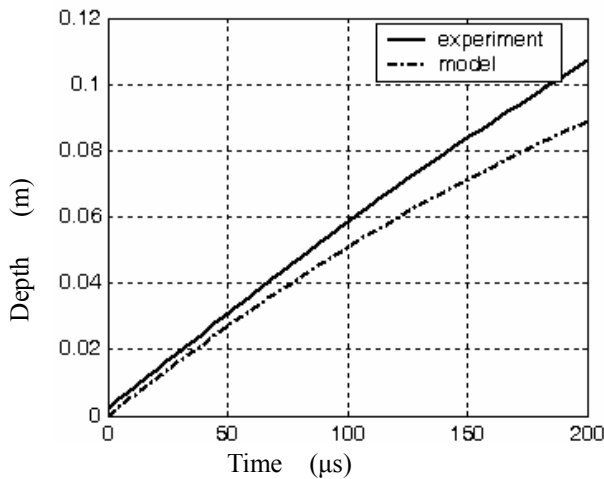


Fig.15 Displacement versus time data and model prediction,  $B=1.0$ ,  $\mu_m=0$ .

## 7 Conclusions

Based on the theoretical analysis and experiment results in this paper, application of this measurement device realized ultra-high  $g$  deceleration-time measurement. It had been demonstrated to function in shock environment up to 145,000  $g$ . The successful design of this device can provide a more effective measurement method for the ultra-high  $g$  penetration test.

For future work, more experiments for the penetration into different material targets are very necessary. Those experiment results can be used to optimize the ultra-high  $g$  deceleration-time measurement device and the mathematic model of penetration.

### References

[1] Forrestal MJ, Altman BS, Cargile JD, Hanchak SJ. An empirical equation for penetration depth of

- ogive-nose projectiles into concrete targets. *Int J Impact Eng*;15:395–405, 1994.
- [2] Forrestal MJ, Frew DJ, Hanchak SJ, Brar NS. Penetration of grout and concrete targets with ogive-nose steel projectiles. *Int J Impact Eng*, 18:465–76, 1996.
- [3] Frew DJ, Hanchak SJ, Green ML, Forrestal MJ. Penetration of concrete targets with ogive-nose steel rods. *Int J Impact Eng*;21:489–97, 1998.
- [4] Frew DJ, Forrestal MJ, Hanchak SJ. Penetration experiments with limestone targets and ogive-nose steel projectiles. *ASME J Appl Mech*;67:841–5, 2000.
- [5] Piekutowski AJ, Forrestal MJ, Poormon KL, Warren TL. Penetration of 6061-T651 aluminum targets by ogive-nose steel projectiles with striking velocities between 0.5 and 3.0 km/s. *Int J Impact Eng*;23:723–34, 1999.
- [6] Forrestal MJ, Piekutowski AJ. Penetration experiments with 6061-T6511 aluminum targets and spherical-nose steel projectiles at striking velocities between 0.5 and 3.0 km/s. *Int J Impact Eng*;24:57–67, 2000.
- [7] Gomez JT, Shukla A. Multiple impact penetration of semi-infinite concrete. *Int J Impact Eng*, 25:965–76, 2001.
- [8] Byers R K, et al. Dynamic Penetration of Soil Media by Slender Projectiles. *Int J Engng Sci*,16:835~844
- [9] Forrestal M J, Luk V K, 1992. Penetration into Soil Targets. *Int J Engng Sci*,12(3):427~444, 1978.
- [10] Forrestal M J, Frew D J. Penetration of concrete targets with deceleration-time measurements. *International Journal of Impact Engineering*, 28: 479–497, 2003.
- [11] Sandialabnews, VOL.52, NO.3 Febuary 11, 2000, Sandia National Laboratory.
- [12] Wendong Zhang, Jing Zu, etc. The Intelligent Missile Black-Box. *IEEE Transactions on Instrumentation and Measurement*, VOL.44, NO.3, 1995.
- [13] Wendong Zhang. Design Method of Storage Measurement and Its Application. High Education Press of China. ISBN 7-04-010432-6.
- [14] Chen X.W., Li Q.M. Deep penetration of a non-deformable projectile with different geometrical Characteristics. *International Journal of Impact Engineering*. 27 (2002) 619–637.
- [15] Chen X.W., Li Q.M. Perforation of a thick plate by rigid projectiles. *International Journal of Impact Engineering*. 28 (2003) 743–759.
- [16] N. V. Nechitailo, R. C. Batra. Penetration/perforation of aluminum, steel and



tungsten plates by ceramic rods. *Computers & Structures* 1998, 66: 571-583.

[17] Paul A, Ramanurty U. Strain Rate Sensitivity of a Closed-cell Aluminum Foam *J. Material Science and Engineering* 2000; 281:1-7.

[18] Deshpande VS, Fleck N A. High Strain Rate Compressive Behavior of Aluminum Alloy Foam *J. Int J Impact Engng* 2000; 24: 277-298.